LANGMUIR

pubs.acs.org/Langmuir Article

Gas Phase Modification of Silica Nanoparticles in a Fluidized Bed: Tailored Deposition of Aminopropylsiloxane

Amirhossein Mahtabani, Damiano La Zara, Rafał Anyszka, Xiaozhen He, Mika Paajanen, J. Ruud van Ommen, Wilma Dierkes,* and Anke Blume

Cite This: *Langmuir* 2021, 37, 4481−4492 Read Online

ACCESS | Metrics & More | Article Recommendations

ABSTRACT: Functionalized nanoparticles have various applications, for which grafting of a chemical moiety onto the surface to induce/improve certain properties is needed. When incorporated in polymeric matrices, for instance, the modified nanoparticles can alter the interfacial characteristics leading to improvements ofthe macroscopic properties of the nanocomposites. The extent of these improvements is highly dependent on the thickness, morphology and conformity of the grafted layer. However, the common liquid-phase modification methods provide limited control over these factors. A novel gas-phase modification process was utilized, with 3-aminopropyltriethoxysilane (APTES) as precursor, to chemically deposit amino-terminated organic layers on fumed silica nanoparticles in a fluidized bed. A self-limiting surface saturation was achieved when the reaction was done at 200 °C. With this self-limiting feature, we were able to graft multiple layers of aminopropylsiloxane (APS) onto the silica nanoparticles using water as the coreactant. The feasibility of this process was analyzed using thermogravimetric analysis (TGA), diffuse reflectance IR Fourier transform spectroscopy (DRIFTS), X-ray photoelectron spectroscopy (XPS), and elemental analysis (EA). By altering the number of APTES/water cycles, it was possible to control the thickness and conformity of the deposited aminopropylsiloxane layer. This novel approach allows to engineer the surface of nanoparticles, by introducing versatile functionalized layers in a controlled manner.

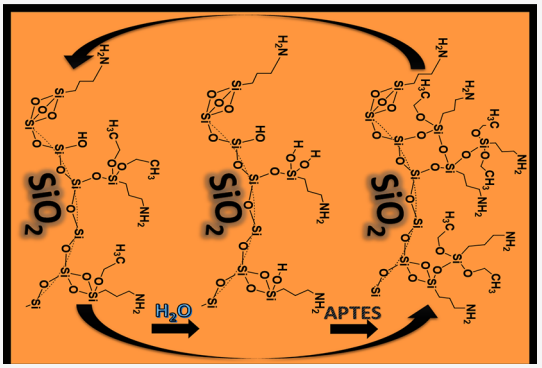

INTRODUCTION

For various industrial and scientific applications, there is a need to functionalize the surfaces of nanoparticles in order to achieve a variety of properties. Among different types of powders, silica nanoparticles are widely used in many fields as filler,[1−3] catalyst carrier,[4] and biological and medical materials.[5] In order to improve the application performance, their surfaces usually need to be modified by functional chemical groups.[6,7] 3-aminopropyltriethoxysilane (APTES) is a commonly used modifying agent because of its versatility and wide application range. Amino-terminated silica particles can be used as filler in rubber and plastic matrices to improve mechanical properties by enhancing the filler−matrix interactions.[8] Amino-terminated silica particles also have a large adsorption capacity and good selectivity for metal ions, such as Cu^{2+}, Pb^{2+}, Hg^{2+}, thus they can be used as chromatography stationary phase or adsorbent.[9−11] Since amino groups can react with proteins and DNA, the functionalized particles have important applications in the separation of biomaterials, enzyme immobilization and targeted medicine.[12,13]

One of the fields where the incorporation of functionalized silica nanoparticles is becoming of growing interest, are high voltage direct current (HVDC) cable insulation systems.[2,3,14] In our previous studies, it was shown that treating silica nanoparticles with APTES results in significant reduction of space charge injection in nanodielectrics under DC fields. This improvement can be due to numerous phenomena, for example, improving filler dispersion,[15] altering the electronic structure at the filler−polymer interface,[16] enhancing nucleation and changing crystalline structures in the semicrystalline polymer matrix.[17] It was also discussed that the amine functional group can induce deep localized states that can trap the "hot" electrons when the DC field is applied.[18] Also, substituting the silanol groups with amine functional groups on the silica can reduce the surface polarity, minimize the dispersion challenges and reduce moisture uptake.[19] Liu et al.[20,21] have shown that the mass of adsorbed moisture and medium sized species, such as byproducts from filler modification and polymer cross-linking, is proportional to

Received: December 28, 2020
Revised: March 23, 2021
Published: April 7, 2021

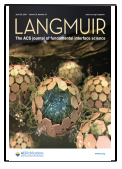

https://doi.org/10.1021/acs.langmuir.0c03647
Langmuir 2021, 37, 4481−4492

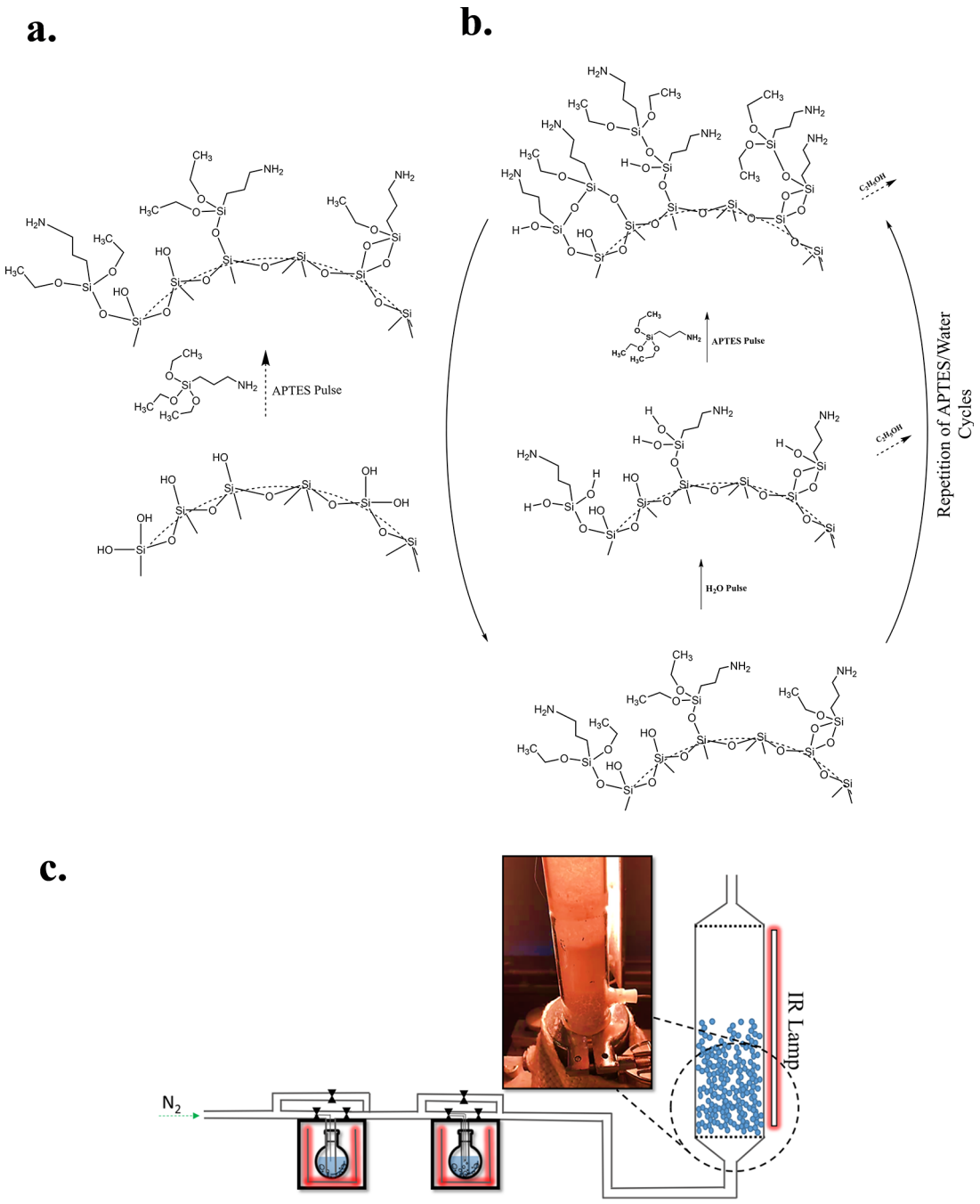

Figure 1. (a) Deposition mechanism of aminopropylsiloxane onto the silica nanoparticles, (b) Repetition of the APTES/water cycles to achieve complete conformal coating of the surface setup.

the hydroxide concentration on the nanoparticle surface. It has also been shown that the long-term deterioration of insulation properties of polymeric nanocomposites can be due to uncontrolled moisture uptake.[22] Therefore, depositing conformal aminopropylsiloxane (APS) layers from APTES on the silica nanoparticles in a controlled manner is a promising way to achieve and maintain good insulation properties.

The preparative method of the functionalized nanoparticles has a remarkable effect on the coating morphology, that is, layer thickness, surface density, orientation of the surface molecules, and the type of interactions between the surface groups and the precursor molecules.[23] Functionalization of nanoparticles is usually done in an aqueous or non-aqueous liquid phase, with organic solvents, for example, toluene, hexane, or ethanol. This method, while proven to be effective,[24] brings about serious issues such as solvent recovery, long operation times, high costs, severe pollution, and low efficiency.[25] Moreover, the presence of water has a great influence on the mechanism of layer formation and further on the structure of the deposited layer.[26] In aqueous conditions, multilayers are formed by oligomerization of bi- and trifunctional alkoxysilanes due to hydrogen-bonding and hydrolysis of precursor molecules before deposition onto the surface via covalent bonds.[23] This usually occurs inevitably and in spite of careful dehydration treatments,[27] hence, making it difficult to control the thickness and morphology of the

https://doi.org/10.1021/acs.langmuir.0c03647
Langmuir 2021, 37, 4481−4492

deposited layers. Elimination of the physisorbed water molecules and deposition of self-saturating molecular layers of alkoxysilanes can be most easily performed in the gas phase. Different silane layers have been deposited onto silica powders in the gas phase by means of carrier particles containing a known quantity of modifying agent.[25,28] However, this approach does not provide control over the thickness and morphology of the deposited layer. Aminosilane layers have been deposited onto silicon dioxide substrates in gas phase via atomic layer deposition (ALD).[29] Hydrolysis of aminosilylated silica, that is hydrolyzing the remaining unreacted alkoxy groups with water, followed by a silanization step resulted in the controlled formation of a high-density amino-terminated siloxane network. When consecutive aminopropyltrialkoxysilane and water cycles have been performed, an increased content of amino groups on porous silica is observed. However, to our knowledge, this approach has not yet been applied on nanoparticles.

In this study, fumed silica nanoparticles were treated in the gas phase in a fluidized bed with 3-aminopropyltriethoxysilane (APTES). APTES reacts with the isolated and geminal silanol groups on the silica in a self-catalyzing manner due to hydrogen bond interactions.[30] Therefore, the first layer can be chemically deposited onto the nanoparticles' surface with no need for hydrolysis. Figure 1a depicts a schematic presentation of this reaction. Different reaction temperatures were applied in order to verify self-limiting surface saturation. Subsequently, multiple layers were deposited onto the nanoparticles via sequential APTES/water cycles (Figure 1b). This process is similar to that of atomic layer deposition (ALD), where layers are formed on a reactive surface by sequential pulses of two precursors in the gas phase. In this way, deposition of APTES can be controlled, layer by layer, by increasing the number of APTES/water cycles. The feasibility of this approach was analyzed using thermogravimetric analysis (TGA), diffuse reflectance infrared Fourier transform spectroscopy (DRIFTS), X-ray photoelectron spectroscopy (XPS), and elemental analysis (EA).

EXPERIMENTAL WORK

Materials. A fumed silica grade, AEROSIL 200 (primary particle size of 7−50 nm) with high purity and low moisture content, was received from Evonik Industries. 3-aminopropyltriethoxysilane (APTES) with 99% purity was purchased from Sigma-Aldrich and used without any further purification. In order to dry the silica, and rule out the effect of air humidity, nanoparticles were kept in an oven at 120 °C for 24 h prior to the modification process.

Gas Phase Deposition of The Silane. The experiments were carried out in a fluidized bed reactor operated at atmospheric pressure: the particles are suspended ("fluidized") in an upward gas flow. The reactor consists of a glass column (2.6 cm in internal diameter and 50 cm in height), placed on top of a double-motor vibration table (Paja PTL 40/40−24) to assist the fluidization process. Two stainless-steel distributor plates with pore size of 37 μm were placed at the bottom and top of the column to obtain a homogeneous distribution of the gas inside the column and to prevent particles from leaving the reactor. APTES was used as the modifying agent and was heated up to 110 °C in a stainless-steel bubbler. In some further experiments, in order to investigate the controllability of the silane layer deposition on the fluidized silica nanoparticles, a second bubbler was added to the setup containing water at room temperature. The bubbler temperature was chosen based on the vapor pressure of the contained substance. The silica nanoparticles were fluidized and pretreated in the glass column with nitrogen (N_2) flow for 1 h at the desired reaction temperature in order to break larger agglomerates of nanoparticles and remove physisorbed water. After the pretreatment, the fluidized powder bed consisted of two zones: a bottom zone with large agglomerates (up to 5 mm in diameter) and a top zone of fine powder, which fluidized smoothly. Subsequently, the fluidized silica was exposed to the precursors carried by nitrogen gas passing through bubblers at different pulse times. After the treatment, the fluidized powder was purged by nitrogen gas to remove byproducts and physisorbed precursor, and the fine powder and agglomerated particles were collected and characterized separately. Since the fine powders are more effectively mixed in the bed, they better represent the properties of the modified nanoparticles with this method, and therefore, are subjected to more detailed characterizations. The details of each experiment are depicted in Table 1.

Table 1. Details of Experiments Performed in the Fluidized Bed

$T_{bubbler}$ (°C)	$T_{reaction}$ (°C)	$t_{pre\text{-}treatment}$ (min)	$t_{reaction}$ (min)	$t_{purging}$ (min)
110	150	60	1	60
			3	
			5	
			10	
	200		1	
			3	
			5	
			10	
	250		1	
			3	
			5	
			10	

It is assumed that upon reaching a surface saturation, there are neither silanol groups on the silica nor hydrolyzed ethoxy groups of already attached silane molecules accessible for the silane to react with. A water pulse through the bed can hydrolyze the remaining ethoxy groups, and result in the growth of the deposited layer upon the next silane pulse. Therefore, it is expected that consecutive APTES/water pulses through the fluidized silica nanoparticles would result in the growth of the deposited layer upon each cycle. Each cycle starts with an APTES pulse for 5 min to deposit a submono layer of the silane onto the fluidized silica nanoparticles. This step is followed by 10 min of nitrogen purging in order to remove the byproducts and the physisorbed APTES. Subsequently, water is sent through the column for 3 min so that the exposed ethoxy groups become hydrolyzed and ready to react with the silane pulsed in the next cycle. Finally, the fluidized silica is purged again with nitrogen for 10 min.

CHARACTERIZATION OF THE NANOPARTICLES

Thermogravimetric Analysis (TGA). In order to estimate the total number of silanol groups on the surface of the nanoparticles, thermogravimetric analysis (TGA 550, TA Instruments) was performed on the untreated Aerosil 200. The method consists of heating up the silica powder from room temperature to 850 °C with a rate of 20 °C/min while measuring the mass loss of the sample. It is assumed that all the physisorbed water is released from the sample up to 150 °C.[31−33] Therefore, the total number of silanol groups for 1 g of silica can be calculated from the mass loss above 150 °C and using eq 1:

https://doi.org/10.1021/acs.langmuir.0c03647
Langmuir 2021, 37, 4481−4492

$$n_{\mathrm{SiOH}}\left(\frac{\mathrm{SiOH}}{\mathrm{nm}^2}\right) = 2\frac{\Delta m \cdot N_A}{M_{H_2O} \cdot S_A} \quad (1)$$

n_{SiOH}: total number of silanol groups, Δm: mass loss in the temperature range: 150 °C < T < 850 °C, N_A: Avogadro's constant, M_{H_2O}: molecular mass of water (18 g/mol), S_A: Surface area of the nanoparticles (200 m^2/g).

The removal of physisorbed water from the nanoparticles is crucial to reach ALD surface saturation. However, the released water from siloxanation of the vicinal silanol groups during the process can hydrolyze and thus initiate oligomerization of the APTES species, and consequently, prevent surface saturation. Therefore, the number of siloxanating silanol groups was estimated at each reaction temperature using TGA: the untreated silica nanoparticles were rapidly (50 °C/min) heated up to the desired temperature, and held isothermally for 1 h. It is assumed that the heating rate during the ramp does not affect the total mass loss up to the isothermal step. The number of silanol groups siloxanating at each temperature can then be calculated from eq 2:

$$n^{T*}_{\mathrm{SiOH}}\left(\frac{\mathrm{SiOH}}{\mathrm{nm}^2}\right) = 2\frac{\Delta m_T \cdot N_A}{M_{H_2O} \cdot S_A} \quad (2)$$

n^{T*}_{SiOH}: number of silanol groups siloxanating at temperature T, Δm_T: mass loss during the isothermal step.

The multiplier two in eqs 1 and 2, is related to the assumption that siloxanation of two adjacent silanol groups results in release of one water molecule.[33] Having calculated the total number of silanol groups as well as the number of silanol groups siloxanating at each reaction temperature, one can calculate the grafting density (GD) of the APTES upon surface saturation using eq 3:

$$\mathrm{GD}^{\mathrm{sat}}_{\mathrm{cal}}\left(\frac{\mathrm{mmolAPTES}}{g\mathrm{silica}}\right) = \frac{n^{T}_{\mathrm{SiOH}} \cdot S_A}{N_A \times 10^{-3}} \quad (3)$$

$n^{T}_{SiOH} = n_{SiOH} - n^{T*}_{SiOH}$, number of remaining silanol groups on the silica at temperature T

GD^{sat}_{cal}: Calculated grafting density of APTES upon saturation

Here, it is assumed that surface saturation takes place in the absence of water, and that in this case, each SiOH reacts only with one APTES molecule, that is, a monodentate structure.[24]

TGA was also performed on the modified silica in order to quantify the level of modification. Each sample was heated up from room temperature to 850 °C with a rate of 20 °C/min. The mass loss above 300 °C was attributed to the thermal decomposition of the aminopropyl groups grafted on the silica surface.[24] The GD can then be calculated from the thermograms according to eq 4:

$$\mathrm{GD}^{\mathrm{sat}}_{\mathrm{exp}}\left(\frac{\mathrm{mmolAPTES}}{g\mathrm{silica}}\right) = \frac{10^3}{M_W}\left(\frac{\Delta W}{1 - \Delta W}\right) \quad (4)$$

GD^{sat}_{exp}: saturated grafting density of APTES from the experiment

$\Delta W\left(\frac{g\mathrm{APS}}{g\mathrm{sample}}\right)$: TGA mass loss between 300 and 850 °C

$1\text{-}\Delta W\left(\frac{g\mathrm{silica}}{g\mathrm{sample}}\right)$: Mass fraction of the pure silica in the modified sample

M_w: Molecular mass of the aminopropyl moiety (58 g/mol).

DRIFTS Measurements. Diffuse reflectance IR Fourier transform spectroscopy (DRIFTS) was utilized to further evaluate the deposition of APTES. Analyses were conducted using a Nicolet 8700 spectrometer (Thermo Fisher Scientific) equipped with a DTGS detector. The samples were prepared using KBr (99+%, FTIR grade, Harrick Scientific Corporation) as background. Spectra were recorded from 4000 to 400 cm^{-1} and averaged over 128 scans, using a resolution of 4.0 cm^{-1}. The data is plotted in the wavenumber range of 4000−1500 cm^{-1} (Figure 4) as this is the range of interest in this case. All the tests were performed at room temperature.

X-ray Photoelectron Spectroscopy (XPS). X-ray photoelectron spectroscopy (XPS) was conducted by means of a PHI Quantera scanning X-ray microscope (USA). It is based on irradiating a material with a beam of X-rays, while simultaneously measuring the kinetic energy and number of electrons that escape from the surface (up to 10 nm in depth) of the material being analyzed. This way, it is possible to measure the elemental composition in parts per thousand (ppt) range covering the surface, with the depth range of a single particle diameter.

Elemental Analysis. Elemental analysis was done using a Thermo Scientific Flash 2000 organic elemental analyzer. Small amounts of the powder were put into tin containers and placed inside the equipment chambers. Subsequently, the sample was heated up until 1000 °C, and the weight percent of present elements was measured.

RESULTS AND DISCUSSIONS

Quantification of The Silanol Groups. Figure 2 shows the thermogram of the untreated silica heated from room temperature to 850 °C. Distinct steps in the mass loss of silica can be observed from the derivative curve. The two steps, reaching their maximum rate first before 100 °C and then around 150 °C, are mainly due to the release of the physisorbed water. This observation validates the assumption used in eq 1, and enables one to calculate the total number of silanol groups on the silica. The mass loss of 1.2% above 150 °C, accounts for 4 SiOH/nm^2 according to eq 1, which is in accordance with what is measured by other methods.[33] According to the mass loss derivative graph in Figure 2, the

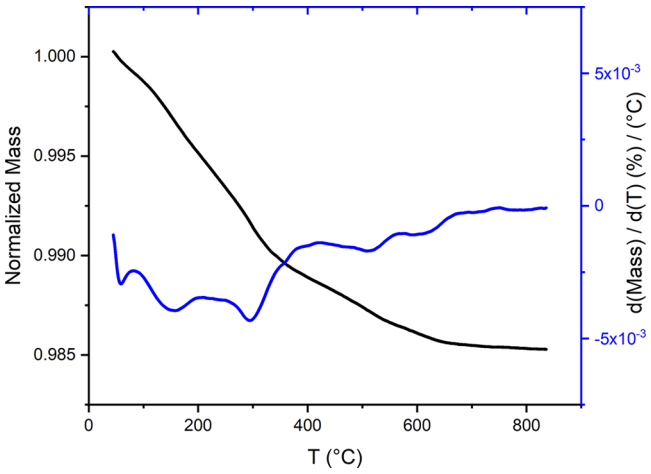

Figure 2. Thermogram of the untreated silica heated from room temperature to 850 °C. Since the mass decreases over time, the derivative curve has negative values

https://doi.org/10.1021/acs.langmuir.0c03647
Langmuir 2021, 37, 4481−4492

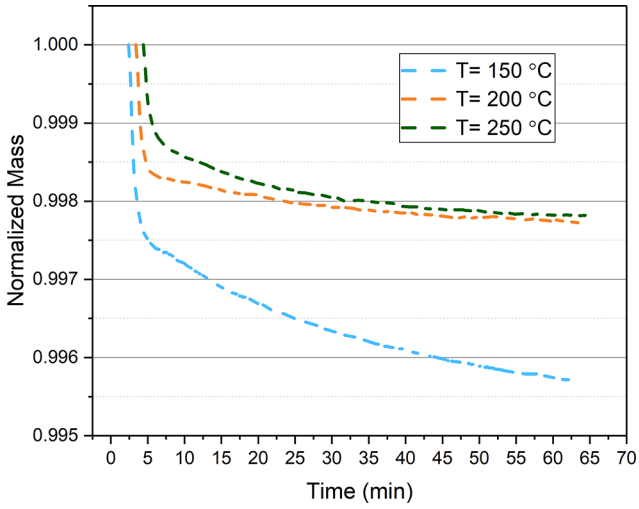

Figure 3. Isothermal thermograms of the untreated silica at three reaction temperatures; the mass loss at 150 °C is significantly higher than the other two temperatures, mainly due to the continuous loss of water from the surface.

release of silanol groups in form of water reaches its maximum rate first around 150 °C and then again around 300 °C. Therefore, in order to avoid APTES oligomerization and reach surface saturation, it is crucial to perform the modification reaction in 150−300 °C temperature range. The high mass loss rate up to 150 °C is mainly due to the release of physisorbed and chemisorbed water. The former is the water directly absorbed to the silica surface, whereas the latter is released as a result of siloxanation of surface silanol groups.[33] The high loss rate at 300 °C is partly associated with the siloxanation of reactive silanol groups, which would substantially decrease the chemical deposition of APS. Therefore, this reaction temperature can be ruled out from the modification experiments. It is also noteworthy here that, according to Wikström et al.[34], no temperature effect on the surface density of amino groups on silica has been observed at reaction temperatures of 120−150 °C, when the deposition of aminosilanes was performed in the gas phase. Therefore, temperatures lower than 150 °C are not necessary to study for this process.

Figure 3 shows the thermograms of untreated silica samples when kept isothermally at each reaction temperature for 1 h.

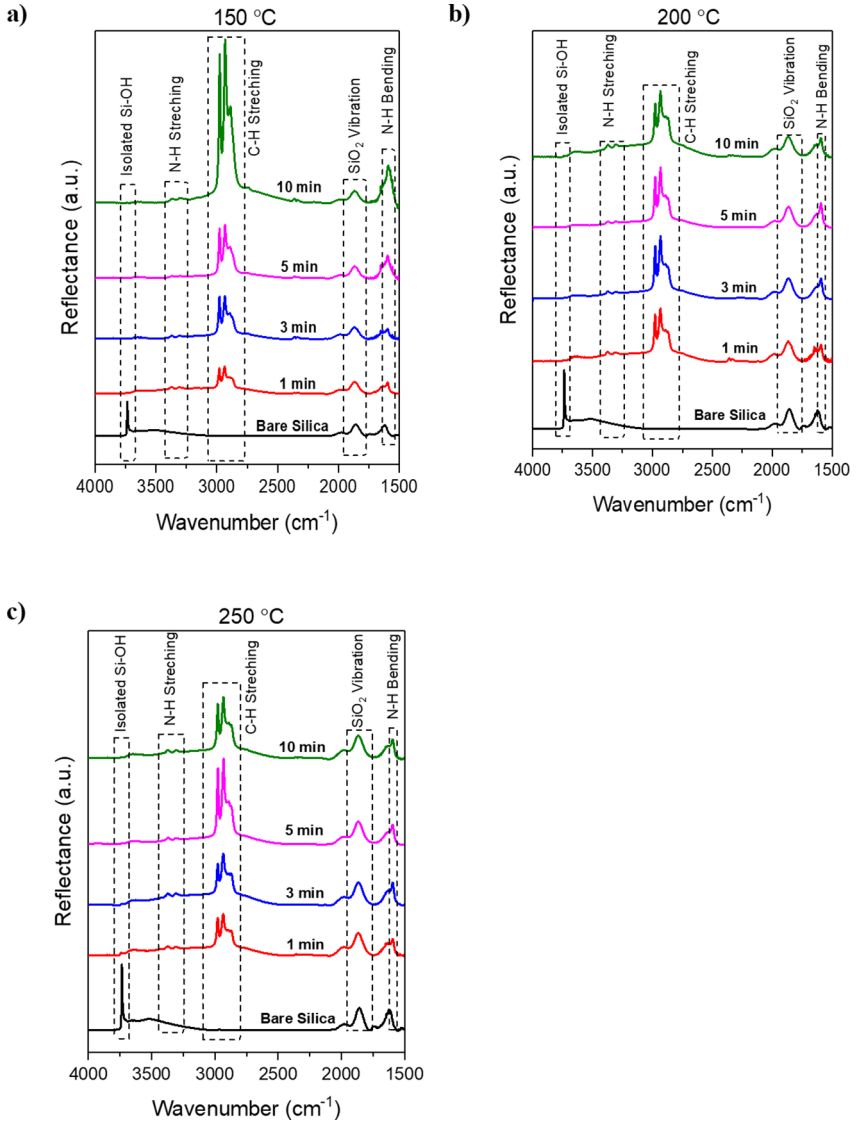

Figure 4. . DRIFTS spectra for all treated silica samples at (a) 150 °C, (b) 200 °C, and (c) 250 °C.

https://doi.org/10.1021/acs.langmuir.0c03647
Langmuir 2021, 37, 4481−4492

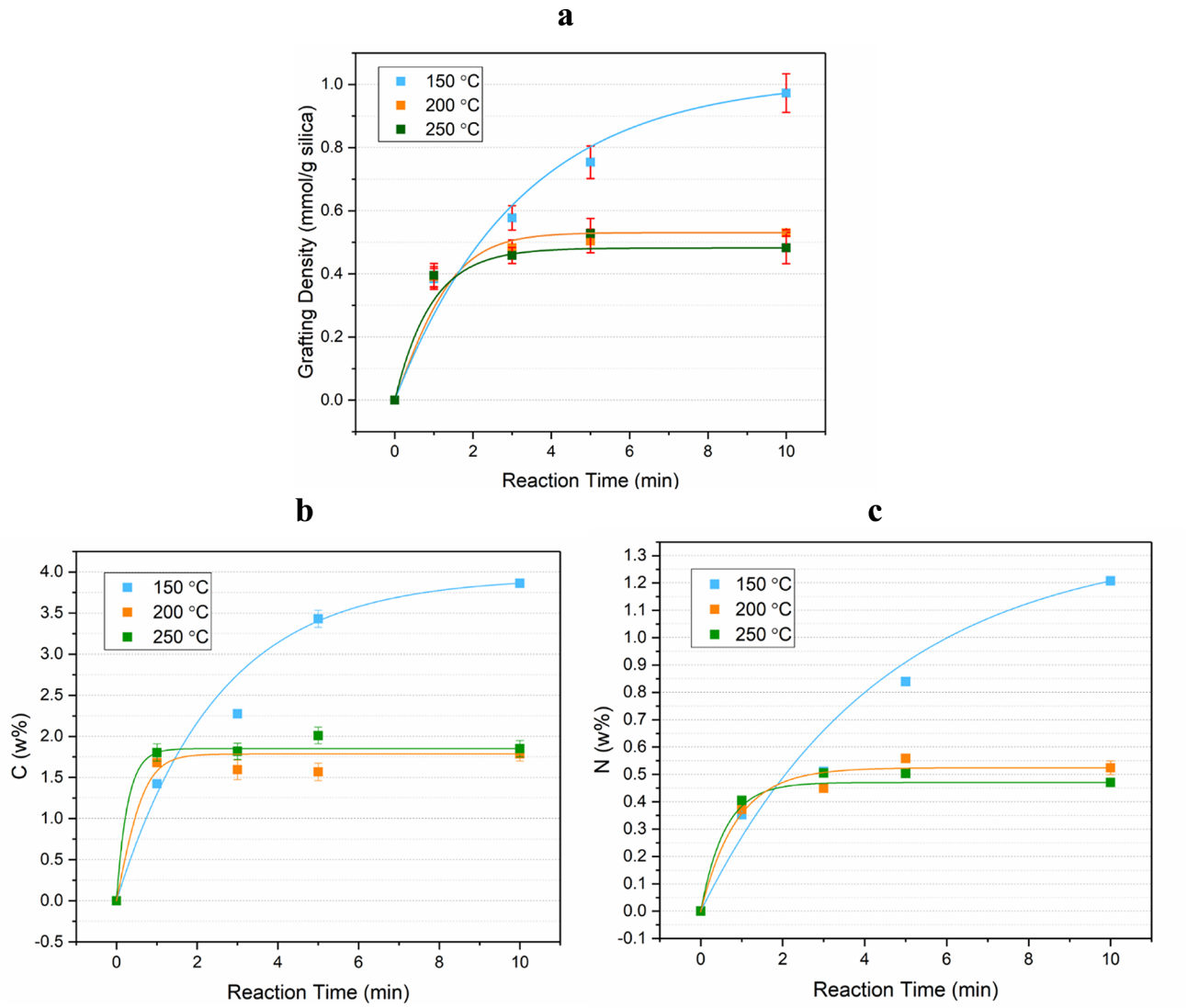

Figure 5. (a) APS grafting densities after 1, 3, 5, and 10 min of precursor pulse time, at three selected temperatures, (b) and (c) carbon and nitrogen content from elemental analysis; the fitted curves are to guide the eye.

Table 2. Number of Silanol Groups and the Calculated and Experimental Values of APS Grafting Density at Three Reaction Temperatures

reaction temperature	$n^{T}_{SiOH}\left(\frac{SiOH}{nm^2}\right)$	$GD^{sat}_{cal}\left(\frac{mmolAPS}{g silica}\right)$	TGA mass loss (%)	$GD^{sat}_{exp}\left(\frac{mmolAPS}{g silica}\right)$	$GD^{sat}_{exp}\left(\frac{APS}{nm^2}\right)$
150 °C	2.56 ± 0.07	0.85 ± 0.02	5.2 ± 0.8	0.97 ± 0.03	2.92 ± 0.09[a]
200 °C	1.79 ± 0.03	0.59 ± 0.01	3.6 ± 0.2	0.51 ± 0.02	1.54 ± 0.06
250 °C	1.05 ± 0.03	0.35 ± 0.01	3.8 ± 0.3	0.52 ± 0.02	1.57 ± 0.06

[a]Since saturation was not achieved at 150 °C, the maximum achieved GD (10 min pulse time) is reported here.

The objective of the isothermal TGA was to determine the lowest temperature range at which the ALD-like saturation is more likely to occur. During the rapid heating, before the stabilization of the temperature, the powder samples lose water; the higher the intended isothermal temperature, the higher the powder loses its physisorbed and chemisorbed water. This can be observed in Figure 3: at 200 °C and 250 °C, less water remains in the sample, hence, the thermograms show lower overall mass loss during the isothermal step compared to 150 °C. This shows that the silica contains relatively more water at 150 °C, and hence, the oligomerization of APTES species during the modification is more likely at this reaction temperature. More so, the mass loss seems not to stabilize throughout the isothermal step, implying that there is still release of water from the silica after being kept at 150 °C for 1 h. Whereas at 200 °C and 250 °C, less water is available on the silica, and mass becomes stable during the isothermal step, indicating more likeliness for surface saturation during the treatment at these reaction temperatures.

Gas-Phase Deposition of the Amino-Silane. Having gained some perspective on the silica, the reaction of vaporized APTES with fumed silica nanoparticles was studied in a fluidized bed using the reaction conditions depicted in Table 1. Three reaction temperatures: 150 °C, 200 °C, and 250 °C,

https://doi.org/10.1021/acs.langmuir.0c03647
Langmuir 2021, 37, 4481−4492

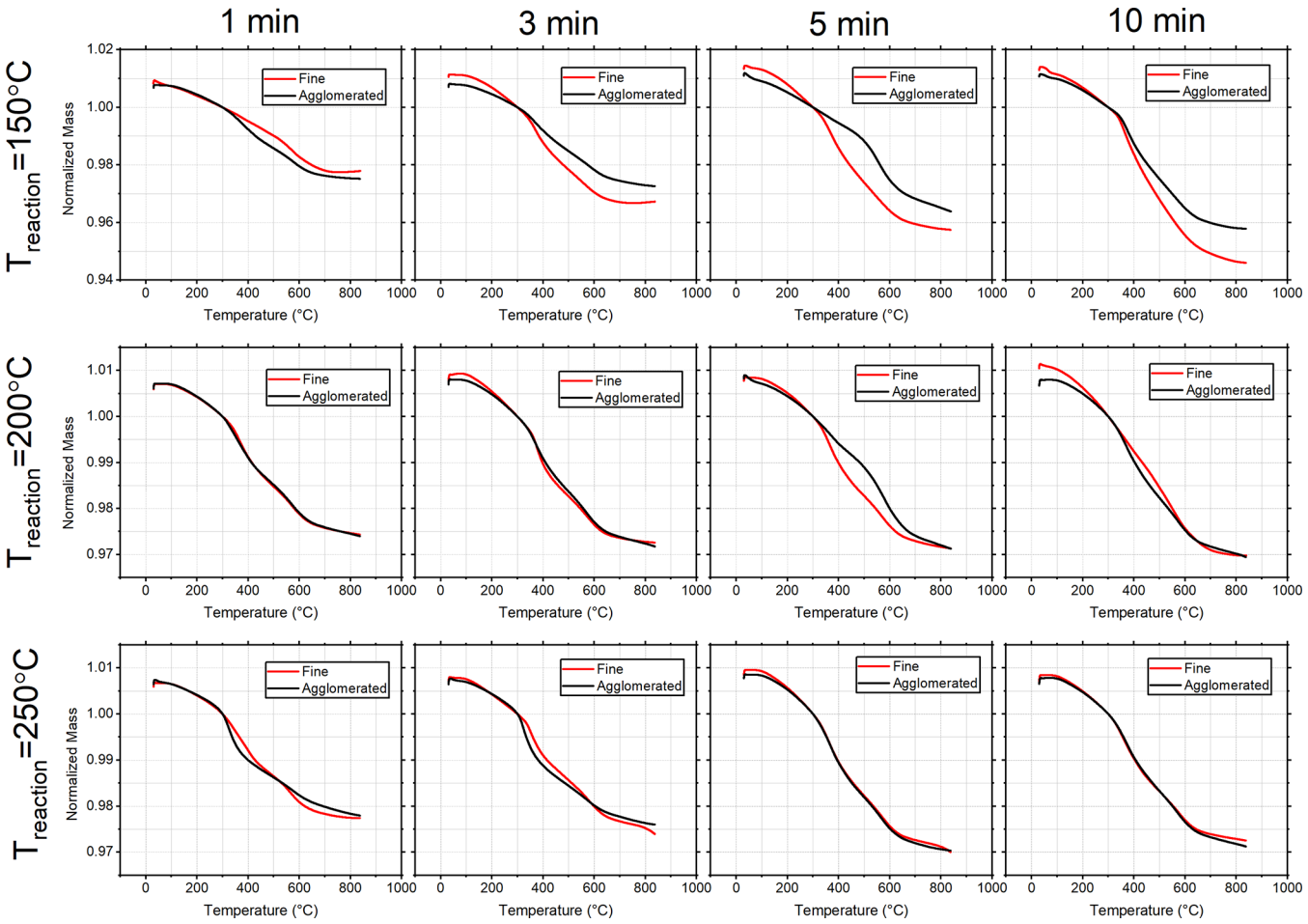

Figure 6. TGA graphs for fine and agglomerated powders of all treated silica samples at different temperatures and reaction times.

were utilized for the process in order to find the temperature at which the reaction is surface-limiting and where conformal self-saturating layers can be formed on the silica surface. This is one of the main features of an ALD process,[35,36] which in this case would enable for controlled deposition of amino-propylsiloxane (APS) on the silica surface. The DRIFTS spectra of all the treated samples compared to the bare silica are presented in Figure 4. All spectra were normalized to the SiO_2 vibrational band at1860 cm^{-1} as the underlying bulk.[37] The isolated Si−OH band at 3750 cm^{-1}, disappearing at pulse times longer than 1 min, regardless of the reaction temperature, indicates the rapid consumption of the isolated silanol groups. This suggests that, after this point, it is mostly the siloxanation of geminal and vicinal silanol groups, that determines the reaction mechanisms. The intensity of the C−H stretching bands at 2870−2970 cm^{-1} increases upon increasing APTES pulse time at 150 °C (Figure 4a), which is not observed in case of 200 and 250 °C. This is an indication of the nonsaturated deposition at 150 °C as opposed to the obtained saturation at higher temperatures. The same increasing trend at 150 °C is observed for the N−H bending band at 1590 cm^{-1}.

The APS grafting densities after 1, 3, 5, and 10 min of precursor pulse time, at three selected temperatures, were calculated based on the TGA results and using eq 4. The results are plotted in Figure 5a. It can be seen that at 150 °C, the silanization reaction is not surface-limiting; the deposited layer keeps growing as the APTES pulse time increases. However, at 200 and 250 °C, the grafting density of the silane reaches saturation at around 0.5 mmol/g silica approximately after 5 min of pulse time. This observation indicates, first, that at 150 °C, the amount of physically and chemically adsorbed water on the silica, which was shown to be higher at this temperature, enables for hydrolyzation of the APTES species and increasing the grafting density with time. This would cause oligomerization of the precursor, and prevents conformal deposition of the APS layer. Instead, at 200 and 250 °C, the absence of the physisorbed water and the lower number of remaining silanol groups prevents APTES oligomerization, resulting in surface saturation after 5 min. This can be an evidence that the APTES precursor has formed a submonolayer of APS on the silica surface preventing any further silanization. The trend for the carbon and nitrogen content is similar to that of the grafting densities estimated from TGA (Figure 5b,c). This confirms that the self-limiting character of this process is valid down to the atomic scale, which is another key feature of an ALD process.

Considering an average of 4 SiOH/nm^2 on the surface of AEROSIL 200 (eq 1), and the number of silanol groups siloxanating at each reaction temperature (eq 2), the saturation grafting density of APS can be estimated (GD^{sat}_{cal} in eq 3) and compared to the experimental value at each reaction temperature (GD^{sat}_{exp} in eq 4). The results are presented in Table 2. The number of reactive silanol groups decreases by increasing the reaction temperature, what is expected as it was observed in form of mass loss in Figure 2. The calculated GD

https://doi.org/10.1021/acs.langmuir.0c03647
Langmuir 2021, 37, 4481−4492

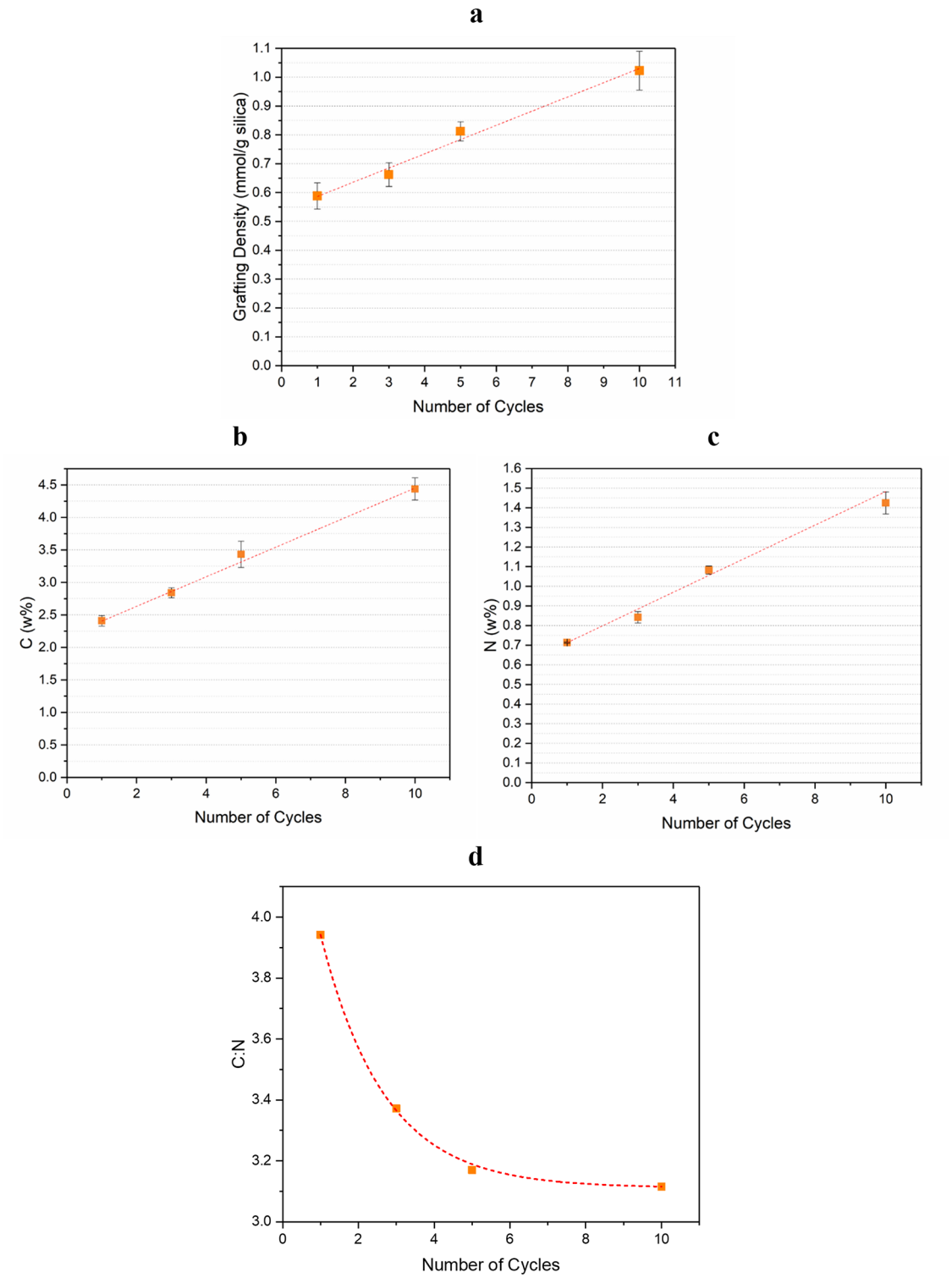

Figure 7. (a) APS grafting densities after 1, 3, 5, and 10 APTES/water cycles, at 200 °C, and (b) carbon, (c) nitrogen content and (d) C:N ratio from elemental analysis.

upon saturation is close to the experimental value when the reaction was performed at 200 °C. An average grafting of 1.54 $\frac{\text{APS}}{\text{nm}^2}$, compared to 1.79 $\frac{\text{SiOH}}{\text{nm}^2}$ available on the silica nanoparticles, implies the formation of an APS submonolayer at 200 °C after 5 min. This also implies that the APTES monodentate structure is more likely to occur at 200 °C, whereas the presence of water at 150 °C, and the promoted condensation at 250 °C may result more in bidentate and tridentate structures.[38] Accordingly, one can estimate that 86% of the silanol groups on the silica have reacted with the silane at 200 °C. This is a significant coverage, for example, compared to the 25% of reacted silanols in case of silanization in silica-filled rubber compounds.[30] A maximum of 2.92 APS molecules are attached per nm^2 of silica at 150 °C, which is on average higher than the number of available SiOH groups on the surface at this temperature. This estimation shows that precursor has

https://doi.org/10.1021/acs.langmuir.0c03647
Langmuir 2021, 37, 4481−4492

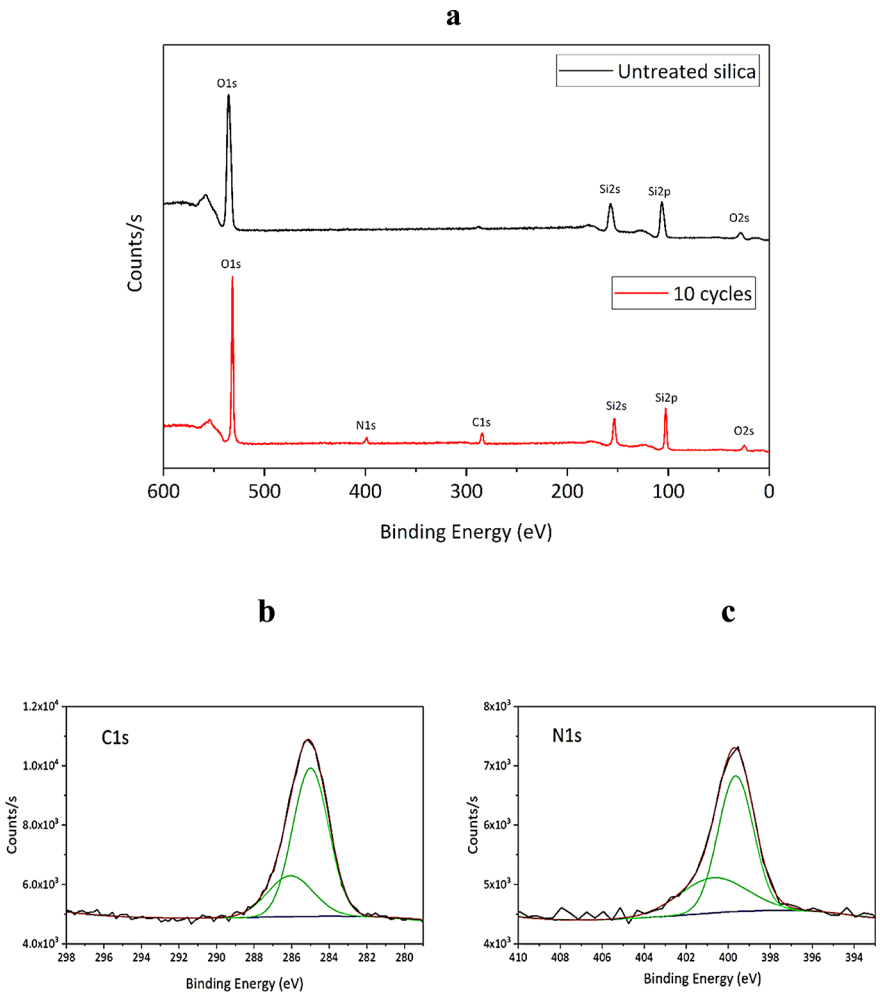

Figure 8. (a) XPS full spectra of the silica sample treated in 10 cycles compared to the untreated reference, (b) and (c) the deconvoluted C 1s and N 1s elemental fine scans for the silica sample treated in 10 cycles.

Table 3. Atomic Percentages of C and N from XPS, Along with C:N Ratios

silica sample	C (at%)	N (at%)	C:N
saturated w/o hydrolyzation	5.35	1.32	4.05
1 cycle	7.63	1.94	3.93
3 cycles	8.33	2.24	3.72
5 cycles	9.13	2.51	3.54
10 cycles	11.34	3.43	3.31

been oligomerized at this reaction temperature. Interestingly, according to these calculations, it seems that the same phenomenon has occurred in case of the reaction at 250 °C. An average of 1.57 $\frac{\text{APS}}{\text{nm}^2}$ is deposited after 5 min of exposure at this temperature, which is higher than 1.05$\frac{\text{SiOH}}{\text{nm}^2}$ available on the surface. This can be due to condensation and cross-linking of APTES species which was shown to be promoted at high reaction temperatures.[38] This effect would result in an increased number of APS grafted onto a unit surface area, compared to the expected value calculated from eq 3. Unlike the reaction at 150 °C, the APS growth mechanism at 250 °C is more affected by horizontal oligomerization of APTES. Nevertheless, despite the condensation effect, the deposition at 250 °C reaches saturation, as the number of silanol groups on the silica is relatively low at such a high temperature.

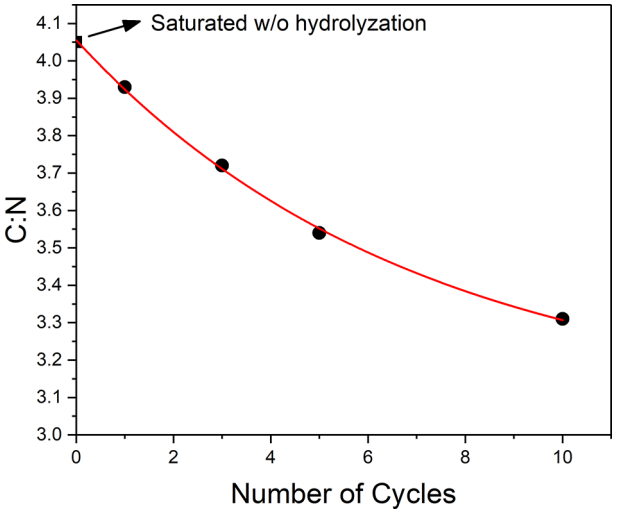

Figure 9. C:N ratio of the silica modified in cycles.

Due to the strong van der Waals forces between silica nanoparticles, agglomeration in a fluidized bed is inevitable.[39] In fact, in contrast to particles in the high micrometer range, nanoparticles are not fluidized individually but as agglomerates: very dilute clusters in the order of 100 μm consisting of billions of primary particles. However, the high van der Waals

https://doi.org/10.1021/acs.langmuir.0c03647
Langmuir 2021, 37, 4481−4492

forces can cause the nanoparticles to form larger agglomerates at the bottom of the fluidized bed column. Grillo et al.[40] demonstrated that despite the agglomerated structure of nanoparticles, surface saturation is feasible even at ambient conditions, which indicates the effective diffusion of the precursor into agglomerates in fluidized bed ALD processes. In our case, large agglomerates, up to 5 mm in diameter, were observed at the bottom of the reactor in all the experiments. Accordingly, it is fair to ask the following question: is the APS deposition conformal, both in the fine fluidized powder and the agglomerates at the bottom of the reactor? Figure 6 shows the TGA graphs for fine and agglomerated powders of all the samples treated at different temperatures and times. In case of reaction temperatures of 200 and 250 °C, the graphs of the fine and agglomerated silica are nearly identical. This indicates that the gas phase deposition of APS is fairly conformal at the temperatures at which surface-limiting behavior takes place. This is another key factor of an ALD process, in which any exposed particle surface with the ability to bond functional groups can be coated, including internal surfaces of porous substrates or agglomerates of nanoparticles.[41] At 150 °C, there is a significant difference between the fine powders and the large agglomerates indicating a nonconformal deposition of APS at this temperature. The fine powder, where primary particles are fully exposed to the gaseous precursors, show higher APTES loadings at this temperature. Whereas, very large nonfluidized agglomerates may suffer from diffusion limitations of the gaseous precursors, thereby preventing a uniform and conformal deposition on each primary particle.[35] It can be seen that this difference tends to be even greater as the reaction time increases implying an increased inhomogeneity in the deposited layer with time.

Repetition of Amino-Silane/Water Cycles. The above results showed that self-limiting APS layers can be deposited onto fluidized silica nanoparticles at 200 °C, reaching a grafting density of ca. 0.5 mmol/g silica after 5 min. The saturation occurs inasmuch as there are no hydrolyzed ethoxy groups accessible anymore at a certain point for the unreacted silane to engage with. Therefore, it is expected that sequential APTES/water pulses through the fluidized silica nanoparticles would result in further growth of the deposited layer upon each cycle.

The APTES grafting density is calculated from TGA data and plotted against the number of APTES/water cycles in Figure 7a. It is clear that increasing the number of cycles results in higher grafting densities of APTES. This confirms that the mechanism shown in Figure 1b is valid for the controlled deposition of the silane: by choosing the appropriate number of cycles, it is possible to reach the desired grafting densities. The above trend is also observed at atomic level as the elemental analysis results show in Figure 7b and 7c: It is perfectly clear that the C and N content follow the same trend as the grafting density does. The C:N ratio decreases by increasing the number of cycles, as it is evident in Figure 7d. The C:N ratio for the unreacted APTES is 9, whereas ideal APS films can be characterized by a C:N ratio of 3, indicative of complete hydrolysis of APTES molecules, and replacement of all ethoxy groups with siloxane bonds. The C:N approaching 3 upon increasing cycles is indicative of a more complete hydrolysis of the precursor.

The XPS spectra of silica samples modified by 10 APTES/water cycles are presented in Figure 8a along with the one of the untreated silica for comparison. The emergence of the peaks corresponding to C 1s and N 1s in the modified silica confirms the presence of APTES on the surface. The deconvoluted elemental fine scans in Figures 8b,c indicate the atomic environment and are dependent on the chemical bonds in the film. As expected, the N 1s fine scan reveals that there are two peaks at 399.6 and 400.7 eV, indicative of C−N and N−H bonds, respectively.[42,43] The C 1s scan also exhibits two peaks, one at 285 eV representing C−C and C−H and at 286.1 eV corresponding to C−N bonds.[42,44]

The atomic percentages of C and N as well as the C:N ratio of the silica modified in cycles are presented in Table 3, along with the modified silica reaching saturation after 5 min of APTES pulse at 200 °C. It is clear that both, the carbon and the nitrogen atom content, increase on the surface of the nanoparticles upon increasing the number of cycles. While this is expected according to the previous test results, the increase in the carbon content should be less significant due to the hydrolysis and release of the ethoxy groups in form of ethanol. This effect is manifested in the decrease in the C:N ratios which was also observed in Figure 7d. The fact that the C:N ratio is closing down to 3 upon increasing the number of cycles (Figure 9), indicates that a conformal APS layer has been formed on the silica nanoparticles, and cross-linked via horizontal siloxanation.

CONCLUSIONS

Controlled deposition of APTES was performed on fumed silica nanoparticles in a fluidized bed. A self-limiting surface saturation, similar to an ALD process, was achieved when the reaction took place at 200 °C. The surface saturation occurring at this temperature was due to the absence of released water from the silica during the process, thus preventing oligomerization of the precursor. With this self-limiting feature, and using water as coreactant, it was possible to hydrolyze the unreacted ethoxy groups in the deposited layer, and hence to chemically graft multiple layers of aminopropylsiloxane onto silica when sequential APTES/water cycles were performed on the fluidized nanoparticles. In this way, it was possible to reach a more complete coating. Increasing the number of cycles resulted in increasing the thickness of the deposited layer enabling for a controlled engineering of the surface of the functionalized nanoparticles.

AUTHOR INFORMATION

Corresponding Author

Wilma Dierkes − *University of Twente, Faculty of Engineering Technology, Department of Mechanics of Solids, Surfaces & Systems (MS3), Chair of Elastomer Technology and Engineering, 7500 Enschede, The Netherlands*;
Email: w.k.dierkes@utwente.nl

Authors

Amirhossein Mahtabani − *University of Twente, Faculty of Engineering Technology, Department of Mechanics of Solids, Surfaces & Systems (MS3), Chair of Elastomer Technology and Engineering, 7500 Enschede, The Netherlands*; orcid.org/0000-0003-2038-012X

Damiano La Zara − *Department of Chemical Engineering, Delft University of Technology, 2629, HZ, Delft, The Netherlands*; orcid.org/0000-0002-0967-7451

Rafał Anyszka − *University of Twente, Faculty of Engineering Technology, Department of Mechanics of Solids, Surfaces &*

https://doi.org/10.1021/acs.langmuir.0c03647
Langmuir 2021, 37, 4481−4492

Systems (MS3), Chair of Elastomer Technology and Engineering, 7500 Enschede, The Netherlands

Xiaozhen He − *University of Twente, Faculty of Engineering Technology, Department of Mechanics of Solids, Surfaces & Systems (MS3), Chair of Elastomer Technology and Engineering, 7500 Enschede, The Netherlands;* orcid.org/0000-0002-9018-9200

Mika Paajanen − *VTT Technical Research Centre of Finland Ltd, FI-33014 Tampere, Finland*

J. Ruud van Ommen − *Department of Chemical Engineering, Delft University of Technology, 2629, HZ, Delft, The Netherlands;* orcid.org/0000-0001-7884-0323

Anke Blume − *University of Twente, Faculty of Engineering Technology, Department of Mechanics of Solids, Surfaces & Systems (MS3), Chair of Elastomer Technology and Engineering, 7500 Enschede, The Netherlands*

Complete contact information is available at: https://pubs.acs.org/10.1021/acs.langmuir.0c03647

Funding

This project has received funding from the European Union's Horizon 2020 research and innovation program under the name of GRIDABLE and the grant agreement No. 720858.

Notes

The authors declare no competing financial interest.

■ ACKNOWLEDGMENTS

We thank Evonik Industries for providing the silica.

■ REFERENCES

(1) Mahtabani, A.; Alimardani, M.; Razzaghi-Kashani, M. Further evidence of filler−filler mechanical engagement in rubber compounds filled with silica treated by long-chain silane. *Rubber Chem. Technol.* **2017**, *90* (3), 508−520.

(2) He, X.; Rytöluoto, I.; Anyszka, R.; Mahtabani, A.; Saarimäki, E.; Lahti, K.; Paajanen, M.; Dierkes, W.; Blume, A. Surface Modification of Fumed Silica by Plasma Polymerization of Acetylene for PP/POE Blends Dielectric Nanocomposites. *Polymers* **2019**, *11* (12), 1957.

(3) Mathabani, A.; Rytöluoto, I.; He, X.; Saarimäki, E.; Lahti, K.; Paajanen, M.; Anyszka, R.; Dierkes, W.; Blume, A. Solution Modified Fumed Silica and Its Effect on Charge Trapping Behavior of PP/POE/Silica Nanodielectrics. *Proceedings of the Nordic Insulation Symposium*, 2019; pp 129−133.

(4) Wang, X.; Lin, K. S. K.; Chan, J. C. C.; Cheng, S. Direct Synthesis and Catalytic Applications of Ordered Large Pore Aminopropyl-Functionalized SBA-15 Mesoporous Materials. *J. Phys. Chem. B* **2005**, *109* (5), 1763−1769.

(5) Li, Y.; Li, N.; Pan, W.; Yu, Z.; Yang, L.; Tang, B. Hollow Mesoporous Silica Nanoparticles with Tunable Structures for Controlled Drug Delivery. *ACS Appl. Mater. Interfaces* **2017**, *9* (3), 2123−2129.

(6) Protsak, I. S.; Morozov, Y. M.; Dong, W.; Le, Z.; Zhang, D.; Henderson, I. M. A 29Si, 1H, and 13C Solid-State NMR Study on the Surface Species of Various Depolymerized Organosiloxanes at Silica Surface. *Nanoscale Res. Lett.* **2019**, *14* (1), 160.

(7) Protsak, I.; Henderson, I. M.; Tertykh, V.; Dong, W.; Le, Z.-C. Cleavage of Organosiloxanes with Dimethyl Carbonate: A Mild Approach To Graft-to-Surface Modification. *Langmuir* **2018**, *34* (33), 9719−9730.

(8) Zhang, L.; Xiong, Y.; Ou, E.; Chen, Z.; Xiong, Y.; Xu, W. Preparation and properties of nylon 6/carboxylic silica nanocomposites via in situ polymerization. *J. Appl. Polym. Sci.* **2011**, *122* (2), 1316−1324.

(9) Oh, S.; Kang, T.; Kim, H.; Moon, J.; Hong, S.; Yi, J. Preparation of novel ceramic membranes modified by mesoporous silica with 3-aminopropyltriethoxysilane (APTES) and its application to Cu2+ separation in the aqueous phase. *J. Membr. Sci.* **2007**, *301* (1), 118−125.

(10) Kłonkowski, A. M.; Grobelna, B.; Widernik, T.; Jankowska-Frydel, A.; Mozgawapar, W. Coordination state of copper(II) complexes anchored and grafted onto the surface of organically modified silicates. *Langmuir* **1999**, *15* (18), 5814−5819.

(11) Jal, P. K.; Patel, S.; Mishra, B. K. Chemical modification of silica surface by immobilization of functional groups for extractive concentration of metal ions. *Talanta* **2004**, *62* (5), 1005−1028.

(12) Kim, J.; Cho, J.; Seidler, P. M.; Kurland, N. E.; Yadavalli, V. K. Investigations of Chemical Modifications of Amino-Terminated Organic Films on Silicon Substrates and Controlled Protein Immobilization. *Langmuir* **2010**, *26* (4), 2599−2608.

(13) Briand, E.; Humblot, V.; Landoulsi, J.; Petronis, S.; Pradier, C.-M.; Kasemo, B.; Svedhem, S. Chemical Modifications of Au/SiO2 Template Substrates for Patterned Biofunctional Surfaces. *Langmuir* **2011**, *27* (2), 678−685.

(14) Dongling, M.; Treese, A. H.; Richard, W. S.; Anna, C.; Eva, M.; Carina, Ö.; Linda, S. S. Influence of nanoparticle surface modification on the electrical behaviour of polyethylene nanocomposites. *Nanotechnology* **2005**, *16* (6), 724.

(15) Khalil, M. S. The role of BaTiO/sub 3/ in modifying the dc breakdown strength of LDPE. *IEEE Trans. Dielectr. Electr. Insul.* **2000**, *7* (2), 261−268.

(16) Ma, D.; Treese, A. H.; Siegel, R.; Anna, C.; Eva, M.; Carina, Ö.; Linda, S. S. Influence of nanoparticle surface modification on the electrical behaviour of polyethylene nanocomposites. *Nanotechnology* **2005**, *16* (6), 724.

(17) Zhang, C.; Mizutani, T.; Kaneko, K.; Mori, T.; Ishioka, M. Space charge behaviors of low-density polyethylene blended with polypropylene copolymer. *Polymer* **2002**, *43* (8), 2261−2266.

(18) Mahtabani, A.; Rytöluoto, I.; Anyszka, R.; He, X.; Saarimäki, E.; Lahti, K.; Paajanen, M.; Dierkes, W.; Blume, A., On the Silica Surface Modification and Its Effect on Charge Trapping and Transport in PP-Based Dielectric Nanocomposites. *ACS Appl. Polym. Mater.* **2020**.23148

(19) Chang, K.-C.; Lin, C.-Y.; Lin, H.-F.; Chiou, S.-C.; Huang, W.-C.; Yeh, J.-M.; Yang, J.-C. Thermally and mechanically enhanced epoxy resin-silica hybrid materials containing primary amine-modified silica nanoparticles. *J. Appl. Polym. Sci.* **2008**, *108* (3), 1629−1635.

(20) Liu, D.; Hoang, A. T.; Pourrahimi, A. M.; Pallon, L. K. H.; Nilsson, F.; Gubanski, S. M.; Olsson, R. T.; Hedenqvist, M. S.; Gedde, U. W. Influence of nanoparticle surface coating on electrical conductivity of LDPE/Al2O3 nanocomposites for HVDC cable insulations. *IEEE Trans. Dielectr. Electr. Insul.* **2017**, *24* (3), 1396−1404.

(21) Liu, D.; Pourrahimi, A. M.; Pallon, L. K.; Sánchez, C. C.; Olsson, R. T.; Hedenqvist, M. S.; Fogelström, L.; Malmström, E.; Gedde, U. W. Interactions between a phenolic antioxidant, moisture, peroxide and crosslinking by-products with metal oxide nanoparticles in branched polyethylene. *Polym. Degrad. Stab.* **2016**, *125*, 21−32.

(22) Nilsson, F.; Karlsson, M.; Pallon, L.; Giacinti, M.; Olsson, R. T.; Venturi, D.; Gedde, U. W.; Hedenqvist, M. S. Influence of water uptake on the electrical DC-conductivity of insulating LDPE/MgO nanocomposites. *Compos. Sci. Technol.* **2017**, *152*, 11−19.

(23) Vansant, E. F.; Van Der Voort, P.; Vrancken, K. C. *Characterization and Chemical Modification of the Silica Surface*; Elsevier, 1995; Vol. *93*.

(24) Qiao, B.; Wang, T.-J.; Gao, H.; Jin, Y. High density silanization of nano-silica particles using γ-aminopropyltriethoxysilane (APTES). *Appl. Surf. Sci.* **2015**, *351*, 646−654.

(25) Lazghab, M.; Saleh, K.; Guigon, P. Functionalisation of porous silica powders in a fluidised-bed reactor with glycidoxypropyltrimethoxysilane (GPTMS) and aminopropyltriethoxysilane (APTES. *Chem. Eng. Res. Des.* **2010**, *88* (5−6), 686−692.

(26) Krasnoslobodtsev, A. V.; Smirnov, S. N. Effect of water on silanization of silica by trimethoxysilanes. *Langmuir* **2002**, *18* (8), 3181−3184.

(27) Moon, J. H.; Shin, J. W.; Kim, S. Y.; Park, J. W. Formation of uniform aminosilane thin layers: an imine formation to measure relative surface density of the amine group. *Langmuir* **1996**, *12* (20), 4621−4624.
(28) Lazghab, M.; Saleh, K.; Guigon, P. A new solventless process to hydrophobize silica powders in fluidized beds. *AIChE J.* **2008**, *54* (4), 897−908.
(29) Ek, S.; Iiskola, E. I.; Niinistö, L.; Vaittinen, J.; Pakkanen, T. T.; Keränen, J.; Auroux, A. Atomic layer deposition of a high-density aminopropylsiloxane network on silica through sequential reactions of γ-aminopropyltrialkoxysilanes and water. *Langmuir* **2003**, *19* (25), 10601−10609.
(30) Blume, A.; Jin, J.; Mahtabani, A.; He, X.; Kim, S.; Andrzejewska, Z. In *New Structure Proposal for Silane Modified Silica*; International Rubber Conference, IRC 2019: London, 2019.
(31) Ek, S.; Root, A.; Peussa, M.; Niinistö, L. Determination of the hydroxyl group content in silica by thermogravimetry and a comparison with 1H MAS NMR results. *Thermochim. Acta* **2001**, *379* (1), 201−212.
(32) Morrow, B. A.; McFarlan, A. J. Infrared and gravimetric study of an aerosil and a precipitated silica using chemical and hydrogen/deuterium exchange probes. *Langmuir* **1991**, *7* (8), 1695−1701.
(33) Mueller, R.; Kammler, H. K.; Wegner, K.; Pratsinis, S. E. OH Surface Density of SiO2 and TiO2 by Thermogravimetric Analysis. *Langmuir* **2003**, *19* (1), 160−165.
(34) Wikström, P.; Mandenius, C. F. Larsson, P.-o., Gas phase silylation, a rapid method for preparation of high-performance liquid chromatography supports. *J. Chromatogr. A* **1988**, *455*, 105−117.
(35) Zhang, D.; La Zara, D.; Quayle, M. J.; Petersson, G.; van Ommen, J. R.; Folestad, S. Nanoengineering of crystal and amorphous surfaces of pharmaceutical particles for biomedical applications. *ACS Appl. Bio Mater.* **2019**, *2* (4), 1518−1530.
(36) Grillo, F.; La Zara, D.; Mulder, P.; Kreutzer, M. T.; Ruud van Ommen, J. Oriented Attachment and Nanorod Formation in Atomic Layer Deposition of TiO2 on Graphene Nanoplatelets. *J. Phys. Chem. C* **2018**, *122* (34), 19981−19991.
(37) Gorski, D.; Klemm, E.; Fink, P.; Hörhold, H.-H. Investigation of quantitative SiOH determination by the silane treatment of disperse silica. *J. Colloid Interface Sci.* **1988**, *126* (2), 445−449.
(38) Yang, S.-q.; Yuan, P.; He, H.-p.; Qin, Z.-h.; Zhou, Q.; Zhu, J.-x.; Liu, D. Effect of reaction temperature on grafting of γ-aminopropyl triethoxysilane (APTES) onto kaolinite. *Appl. Clay Sci.* **2012**, *62*−*63*, 8−14.
(39) van Ommen, J. R.; Valverde, J. M.; Pfeffer, R. Fluidization of nanopowders: a review. *J. Nanopart. Res.* **2012**, *14* (3), 737.
(40) Grillo, F.; Kreutzer, M. T.; van Ommen, J. R. Modeling the precursor utilization in atomic layer deposition on nanostructured materials in fluidized bed reactors. *Chem. Eng. J.* **2015**, *268*, 384−398.
(41) King, D. M.; Liang, X.; Weimer, A. W. Functionalization of fine particles using atomic and molecular layer deposition. *Powder Technol.* **2012**, *221*, 13−25.
(42) Yan, X.; Xu, T.; Chen, G.; Yang, S.; Liu, H.; Xue, Q. Preparation and characterization of electrochemically deposited carbon nitride films on silicon substrate. *J. Phys. D: Appl. Phys.* **2004**, *37* (6), 907−913.
(43) Dementjev, A. P.; de Graaf, A.; van de Sanden, M. C. M.; Maslakov, K. I.; Naumkin, A. V.; Serov, A. A. X-Ray photoelectron spectroscopy reference data for identification of the C3N4 phase in carbon−nitrogen films. *Diamond Relat. Mater.* **2000**, *9* (11), 1904−1907.
(44) Endo, K.; Maeda, S.; Aida, M. Simulation of C1s Spectra of C- and O-Containing Polymers in XPS by ab initio MO Calculations Using Model Oligomers. *Polym. J.* **1997**, *29* (2), 171−181.

https://doi.org/10.1021/acs.langmuir.0c03647
Langmuir 2021, 37, 4481−4492